GEOPHYSICS, VOL. 65, NO. 4 (JULY-AUGUST 2000); P. 1168–1178, 14 FIGS.

Fresnel zones and spatial resolution for *P*- and *SH*-waves in transversely isotropic media

Patrick N. Okoye* and Norm F. Uren*

ABSTRACT

In an elastically anisotropic medium where the seismic wave velocity is a function of direction, the wavefront shape is nonspherical and, in most cases, assumes a nonelliptical shape. Numerical modelling techniques have been used to calculate the Fresnel-zone diameter for compressional (P) and shear (SH) waves in transversely isotropic and isotropic media, respectively. The size of the Fresnel zone is found to be predominantly dependent on the curvatures and wavelength of the wavefront as well as the dip angle of the reflector. In addition, the anisotropic elastic parameters δ^* (critical near-vertical anisotropy), ε (the P-wave anisotropy), and γ (the SH-wave anisotropy) are found to significantly affect the size of the Fresnel zone.

Numerical modeling results show considerable differences between the Fresnel zones for anisotropic and isotropic velocity functions at various reflector dips. In addition, the Fresnel-zone dimensions for anisotropic media exhibit asymmetry and considerable change with dip. By way of contrast, those of the corresponding isotropic velocity field exhibit symmetry and negligible variation with dip. The spatial resolution of unmigrated seismic data in an anisotropic medium would consequently be significantly different from that determined for the same medium if it is assumed to be isotropic.

Physical modeling results demonstrate that anisotropy can significantly affect the spatial resolving power of seismic waves. The degree of these effects depends on the wavefront curvature, which changes with dip and orientation of the symmetry axis. This observation indicates that the spatial imaging of unmigrated reflection events from the base of thick shale sediments will be affected by anisotropy.

INTRODUCTION

The size or extent of the Fresnel zone determines the spatial resolving power for unmigrated seismic data with which important lithological changes along a seismic profile direction may be observed. Wave theory tells us that a finite area of a reflector is involved in a reflection that gives rise to an event on the seismic trace. This area is called the Fresnel zone and is equal to the region of constructive reflection interference surrounding the geometrically predicted reflection point. The concept of an area, rather than a point on the reflector, being involved in reflection is the essence of spatial resolution. The Fresnel-zone concept thus forms a basis of wave physics and plays an important role in the formation of the field at an observation point. The actual field-formation region is finite despite the presence of infinitely extended "tails" in the Fresnel zone (Asatryan and Kravtsov, 1988).

Huygens's principle for elastic waves indicates that each point on a scattering surface behaves like a source of secondary P- and S-wavefronts. Hence, the wave-theoretical reflection response can be evaluated by summing over the entire scattering surface. Some parts of this surface integral sum constructively, whereas other parts sum destructively (Eaton et al., 1991). The Fresnel zone can be defined as the region of constructive interference enclosing the ray-theoretical reflection point (Sheriff, 1980). The Fresnel zone plays an important role in the solution of many wave propagation problems. Seismic interpreters often use the Fresnel-zone concept to estimate the lateral resolution of unmigrated, stacked seismic data. Attention to the Fresnel zone has been increasing as more effort is devoted to improving seismic resolution. Resolution in a 3-D sense incorporates not only the vertical resolution but also the horizontal resolution. Improving one automatically improves the other (Lindsey, 1989).

Numerical modeling techniques are used here to study the Fresnel-zone diameter in anisotropic media for both P- and SH-waves. A zero source-receiver offset configuration was used and the Fresnel zone determined at different reflector dip angles. The 3-D modeled reflecting interface (Figure 1)

Manuscript received by the Editor September 8, 1998; revised manuscript received August 19, 1999.
*Curtin Univ. of Technology, Dept. of Exploration Geophysics, New Technologies Bldg., Kent Street, Bentley, Perth, Western Australia 6845, Australia. E-mail: patrick@geophy.curtin.edu.au; uren@geophy.curtin.edu.au.

is situated at a specified depth below a transversely isotropic medium. The measured values of anisotropic parameters in sedimentary rocks (Thomsen, 1986) were used in carrying out this study. The different values of the elastic parameters used here represent the extreme values measured for other anisotropic sedimentary rocks. Strong anisotropy, characterised by high values of the P-wave anisotropy, ε, and the near-vertical anisotropy, δ^*, can be too extreme to be representative of common geological media in seismic prospecting. The use of extreme cases, however, clearly demonstrates the main effects of anisotropy on Fresnel-zone dimensions and hence spatial resolution. The generality and practical applications of the results of the numerical research are made clearer by varying the anisotropic parameters ε, δ^*, and γ for P- and SH-waves for chosen anisotropic rocks, and examining the effects on Fresnel-zone diameter at varying reflector dip angles. Results obtained indicate that changes in the elastic parameters considerably influence the Fresnel-zone size and hence horizontal resolution. Physical modeling experiments were also conducted in order to demonstrate the effects of elastic anisotropy on spatial resolution.

GEOMETRY OF FRESNEL ZONES

Wavefronts rather than rays are adopted in the diagrammatic approach to Fresnel-zone calculation in this paper. This simplified concept, apart from possessing better physical meaning, is largely self-explanatory. It also demonstrates how variations in wavefront curvature in the presence of anisotropy affect the Fresnel-zone diameter and hence resolution.

Figure 2a shows an isotropic wavefront incident on horizontal and dipping reflectors respectively. S is a coincident source and receiver, Z is the reflector depth, and R_1 and R_2 the radii of the first Fresnel zone. The limit of constructively interfering reflection response is the locus of points on the reflection surface where the increase in one-way path length from the centroid is one-quarter wavelength. The distance H, from the source (S) to the edge of the Fresnel zone will thus be equal to

$$H = Z + \lambda/4, \tag{1}$$

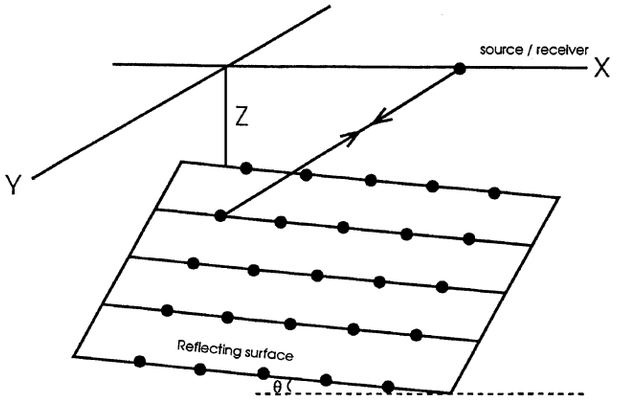

FIG. 1. A simplified geometry of the ray path for reflection from a gridded 3-D tilted surface. The reflecting surface dips at an angle θ in the positive X direction. Traveltimes from the source/receiver to the surface are calculated for each grid point (finely spaced at 1 m intervals).

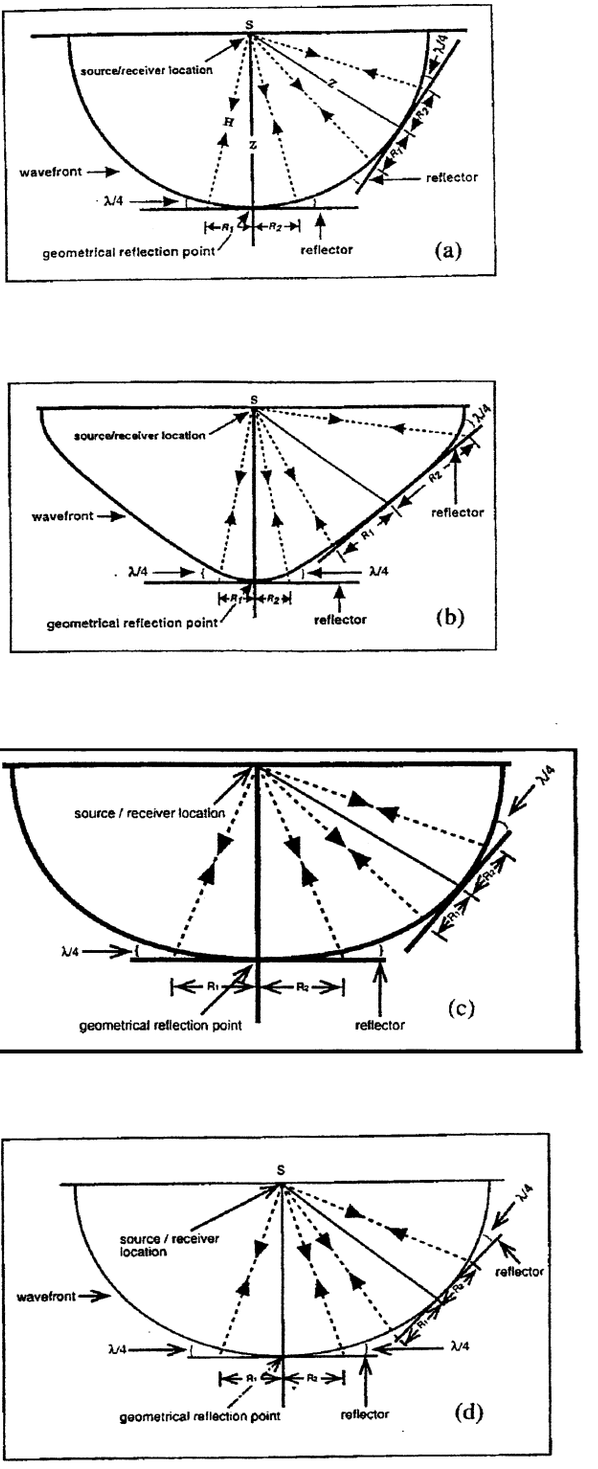

FIG. 2. Numerical approach to Fresnel-zone diameter determination from horizontal and dipping interfaces using seismic wavefronts: (a) spherical wavefront, (b) Nonspherical P-wavefront in Green River shale, negative δ^*, (c) nonspherical P-wavefront in Mesaverde clayshale, positive δ^*, and (d) nonspherical SH-wavefront in Green River shale. This simplified approach demonstrates how variations in wavefront curvature may affect Fresnel-zone diameter and hence resolution for unmigrated data.

where λ is the wavelength of the wave. Using Pythagoras's theorem,

$$(Z + \lambda/4)^2 = Z^2 + R^2. \tag{2}$$

Solving for $R = R_1 = R_2$ gives

$$R = (\lambda Z/2 + \lambda^2/16)^{1/2}. \tag{3}$$

Assuming $Z \gg \lambda$, then the Fresnel radius R will be given by

$$R \approx (\lambda Z/2)^{1/2} \tag{4}$$

Equation (4) can also be expressed in terms of velocity V, frequency F, and arrival time t as

$$R \approx V/2(t/F)^{1/2}. \tag{5}$$

Due to the spherical nature of the wavefront in an isotropic medium, the portions of the horizontal and dipping reflectors in contact with the incident wavefront are equal. Hence, the Fresnel radii will not be expected to change with reflector dip angle.

Figure 2b illustrates the same approach to Fresnel-zone estimation for a nonspherical P-wavefront for both horizontal and dipping reflectors. The wavefront represents that in Green River shale having a negative value of δ^*. This figure shows the contrasting curvatures of the wavefront incident on the horizontal and dipping reflectors. The wavefront incident on the horizontal reflector is clearly less oblate than that on the dipping reflector. Therefore, since a smaller area of the horizontal reflector is in contact with the wavefront, the Fresnel-zone diameter for the horizontal reflector is smaller than that of the dipping reflector.

The Fresnel zone estimation using Mesaverde clayshale with a positive and high value of δ^* is shown in the Figure 2c. Due to the positive value of δ^*, the wavefront is more oblate at horizontal and near vertical directions. Hence, the portions of the horizontal and dipping reflectors in contact with the wavefront are different, demonstrating that the Fresnel-zone diameter and hence spatial resolving power of an anisotropic wavefront depend on the wavefront curvature and dip angle of the reflector. The elastic parameters used in generating these wavefront shapes are taken from Thomsen (1986), which provided information on the elastic properties of representative anisotropic sedimentary rocks. The elastic parameter δ^* controls the wavefront shape without affecting either the vertical or the horizontal velocity values (Okoye, 1995)

VELOCITY FUNCTION GENERATION

The numerical modeling studies carried out here employ anisotropic velocity functions in theoretical ray tracings and Fresnel-zone calculations. This required the computation of both the phase and ray velocities for selected anisotropic rocks used as representative examples. The computed velocity functions are implemented as function subprograms in the program.

Thomsen (1986) gives the expression for the ray velocity $V(\phi)$ in terms of the phase velocity $v(\theta)$ in the form

$$V^2(\phi(\theta)) = v^2(\theta) + \left(\frac{\partial v}{\partial \theta}\right)^2, \tag{6}$$

where ϕ is the ray angle from the source point to the wavefront measured with respect to the symmetry axis and gives the direction of energy propagation. The phase angle θ is the angle between the wavefront normal and the axis of symmetry.

The P- and SH-wave phase velocity expressions are given by

$$v_p^2(\theta) = \alpha_o^2[1 + \varepsilon \sin^2\theta + D^*(\theta)] \tag{7}$$

and

$$v_{SH}^2(\theta) = \beta_o^2[1 + 2\gamma \sin^2\theta], \tag{8}$$

where

$$D^*(\theta) \equiv \frac{1}{2}\left(1 - \frac{\beta_o^2}{\alpha_o^2}\right)\left\{\left[1 + \frac{4\delta^*}{\left(1 - \beta_o^2/\alpha_o^2\right)^2}\sin^2\theta\cos^2\theta + \frac{4\left(1 - \beta_o^2/\alpha_o^2 + \varepsilon\right)\varepsilon}{\left(1 - \beta_o^2/\alpha_o^2\right)^2}\sin^4\theta\right]^{1/2} - 1\right\}. \tag{9}$$

where, α_o = vertical P-wave velocity, β_o = vertical SH-wave velocity, and δ^* = the critical near-vertical anisotropy (a combination of elastic constants).

The computational procedure, though analytical in principle, requires numerical implementation. A quadrant of 800 values of ray velocity was computed at constant increments of phase angle θ and tabulated against the corresponding values of ϕ. From the tabulated values of $V(\phi)$ and ϕ, the ray velocity at the required angle ϕ was found by four-point Lagrangian interpolation. This technique is applicable to both P- and SH-waves.

RAY TRACING AND CALCULATION OF THE FRESNEL-ZONE DIAMETER

Assuming a transversely isotropic medium, the wave surfaces of SH-waves are ellipsoids of rotation, but those for P- and SV-waves are not, in general. Consequently, the method of images (Dellinger and Muir, 1988) is inappropriate for P- and SV-waves. Rather, a more general approach was adopted for the ray tracing and determination of the Fresnel-zone sizes.

An iterative method (Okoye, 1995) based on Fermat's principle was used to find the path of least reflected traveltime. A similar procedure was adopted in determining the reflection time at the edge of the Fresnel zone, which is defined in terms of the chosen center frequency for an assumed seismic wavelet. The search for this time starts from the determined geometrical reflection point with small increments on the reflector of not more than 1 m. This procedure continues until the computed time is equal to the time at the edge of the Fresnel zone.

NUMERICAL MODELING RESULTS

Isotropic and anisotropic Fresnel-zone diameter

Figure 3 shows the plot of normalized P-wave Fresnel-zone diameter versus reflector dip angle using anisotropic Green River shale ($\delta^* = -0.45$) and Mesaverde clayshale ($\delta^* = 0.818$) velocity functions. The Fresnel-zone diameters have been normalized with respect to the equivalent isotropic Fresnel-zone diameter in each case. These two anisotropic rocks have radically different velocity characteristics. These examples

show that the Fresnel-zone diameter in anisotropic media are marked by significant changes at different attitudes of the reflector. Consequently, the spatial resolution in anisotropic media would be expected to change, depending on the dip angle of the reflector. Due to the spherical nature of the isotropic P-wavefront, the Fresnel-zone diameter exhibited no variation with dip. Whether the resolution will be enhanced or reduced depends on the value and sign of the elastic parameter δ^*, which controls the wavefront shape at oblique angles.

Isochronal representations of the P-wave reflections at dip across the Fresnel-zone diameter are shown in Figure 4 using isotropic and anisotropic Green River shale velocity functions. The isotropic reflection isochrons show that the reflection patterns returning from the plane surface are circles expanding from a fixed center with increasing time. Hence, for coincident source and receiver, the Fresnel-zone shape in this case will be circular. By contrast, the anisotropic reflection isochrons assume a more complex shape with dip, and the reflection isochrons are nonsymmetric in nature. The nonsymmetric nature of the anisotropic Fresnel radii with dip indicates that the concept of a single radius and circular Fresnel zone is inappropriate in the presence of anisotropy.

Figure 5 shows the plot of SH-wave Fresnel-zone diameter versus reflector dip obtained assuming isotropy ($\gamma = 0$) in Green River shale and using the anisotropic Green River shale velocity function. This figure also shows that the isotropic SH-wave Fresnel zones are invariant with changes in reflector dips, the same as for the isotropic P-wave case. The anisotropic SH Fresnel zones show no significant changes with dip. This is attributed to the nearly spherical shape of the anisotropic SH-wavefront (Figure 2d) as a result of its low value of SH-wave anisotropy γ. The pertinent question to be addressed is, if γ were larger, will the Fresnel-zone diameter be affected and

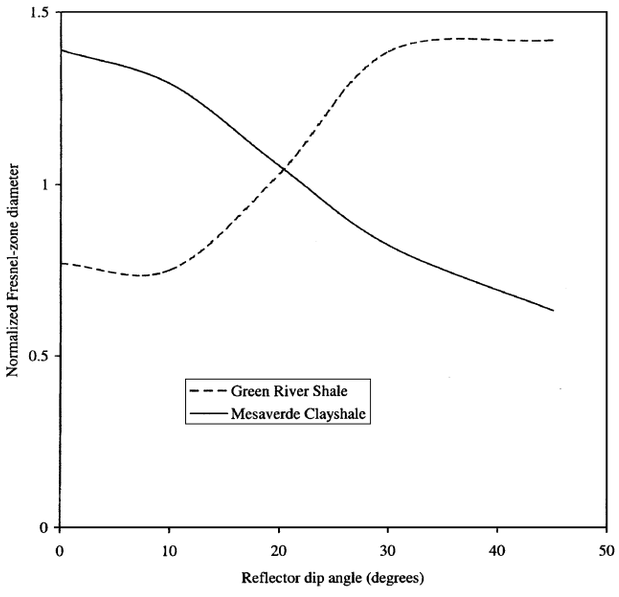

FIG. 3. Normalized P-wave Fresnel-zone diameter plotted as a function of reflector dip angle using Green River shale (negative δ^*) and Mesaverde clayshale (positive δ^*) as numerical examples. The Fresnel-zone diameter exhibits significant changes with reflector dip angle. The Fresnel-zone diameters have been normalized with respect to the equivalent isotropic values, which do not vary with dip due to the spherical nature of the wavefront in isotropic medium.

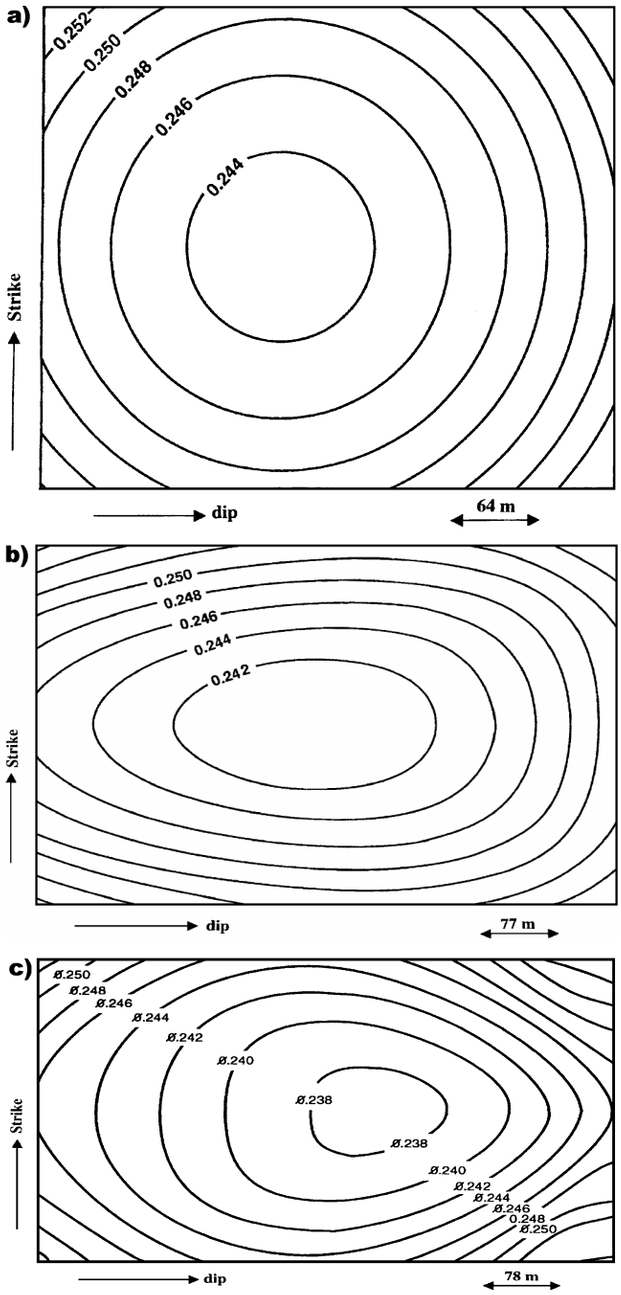

FIG. 4. (a) Isotropic reflection isochrons across the Fresnel-zone diameter from the reflecting surface dipping at an angle of 30°. The diameter of the Fresnel-zone spans 423 m. The circular and concentric behavior of the isochrons still remain unchanged with dip, although the center of the reflection patterns have been shifted updip. (b) Anisotropic reflection isochrons across the Fresnel-zone diameter from the reflecting surface dipping at an angle of 30°. The diameter of the Fresnel-zone spans 581 m. The reflection isochrons are clearly seen to be nonspherical and nonsymmetrical, indicating possible variations in shape and size of the Fresnel-zone diameter with dip. (c) Anisotropic reflection isochrons across the Fresnel-zone diameter from the reflecting surface dipping at an angle of 45°. The diameter of the Fresnel-zone spans 594 m. The reflection isochrons assume a more complex shape with increase in dip, and the nonsymmetric nature of the isochrons increase. The distortion of the contours near the corners are an artifact of the contouring package and should be ignored (contour interval 0.002 s).

hence affect the resolving powers of *SH*-waves in anisotropic media? The answers to this question are presented in the results of the next section which deals with the effects of elastic parameters on Fresnel-zone diameter.

ELASTIC PARAMETERS AND FRESNEL-ZONE DIAMETER

The generality and practical applications of the results of the numerical research are made clearer by varying the elastic parameters ε, δ^*, and γ for *P*- and *SH*-waves in the Green River shale model, and examining how they affect the observed Fresnel-zone diameter at varying reflector dip angles.

Effects of variations in ε on Fresnel-zone diameter

Figure 6a shows plots of Green River shale velocity function shapes obtained using different values of *P*-wave anisotropy, ε, while keeping δ^* constant ($\delta^* = -0.45$). This figure indicates that ε has considerable influence on the shapes of the wavefronts. The effect on the Fresnel-zone diameter is presented in Figure 6b. An analysis of this figure leads to the following observations.

At low values of ε, the radius of curvature of the wavefront gets smaller at horizontal and near-vertical directions while broadening at intermediate dips. This explains the low and high values of the Fresnel-zone diameter obtained in these directions. Therefore, for a medium with low *P*-wave anisotropy, spatial resolution is expected to be better for horizontal and low-dipping reflectors than for reflectors dipping at intermediate angles.

At high values of ε, the wavefront becomes more broadened at horizontal and near-vertical directions while attaining a more concave shape at intermediate angles. This similarly leads to a significant increase and decrease in Fresnel-zone dimensions in these directions. This is opposite to the trend obtained with low ε values. Therefore, it seems that if the *P*-wave anisotropy, ε, is high, spatial resolution for horizontal and shallow-dipping reflectors will be reduced relative to the isotropic case. The opposite is expected for reflectors dipping at intermediate angles.

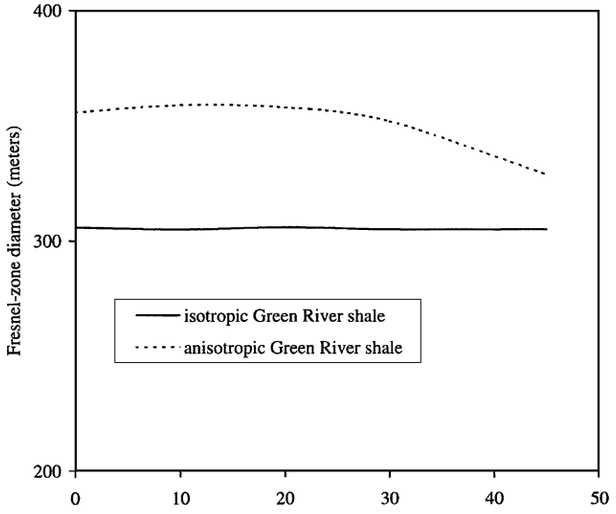

FIG. 5. *SH*-wave Fresnel-zone diameter plotted as a function of reflector dip angle assuming isotropy in Green River shale and using the anisotropic Green River shale velocity function. Due to the nearly spherical shape of the anisotropic *SH*-wavefront, the Fresnel-zone diameter shows no significant variations with dip.

Effects of variations in δ^* on Fresnel-zone diameter

Figure 7a similarly shows plots of Green River shale velocity function shapes obtained using different values of *P*-wave near-vertical anisotropy, δ^*, while keeping ε constant ($\varepsilon = 0.195$). This figure clearly illustrates that this parameter has significant influence on the curvatures of the wavefront. The net effects on the diameter of the Fresnel zone are illustrated in Figure 7b.

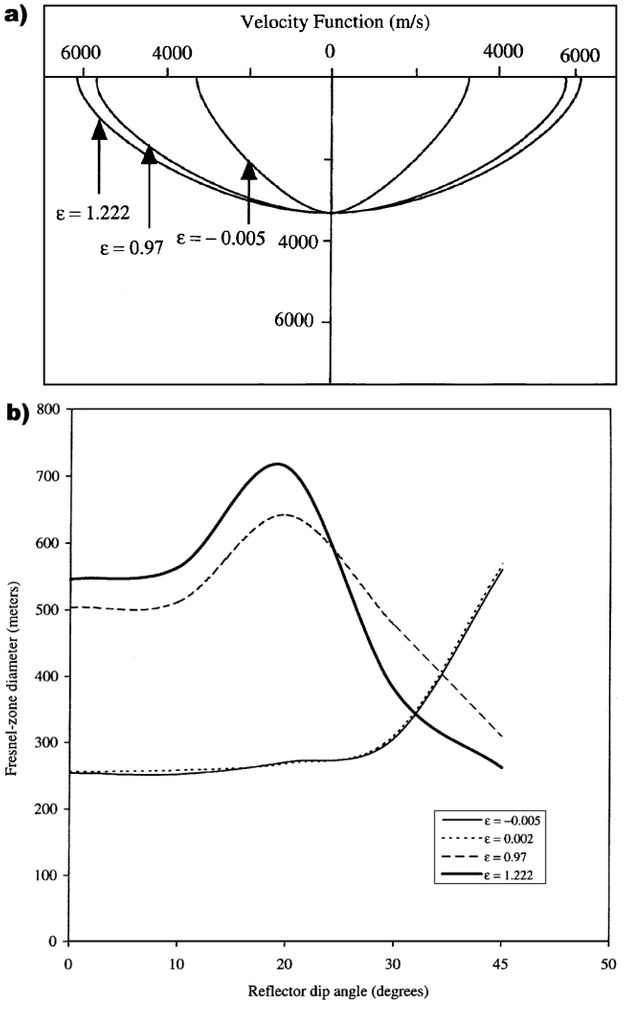

FIG. 6. (a) *P*-group velocity function shapes in Green River shale for different values of ε. Low ε values result in concave wavefront shapes at horizontal and oblique directions, high values of ε give rise to oblate wavefront curvatures in these directions. (A constant value of $\delta^* = -0.45$ was used). (b) *P*-wave Fresnel-zone diameter plotted as a function of reflector dip angle for different values of *P*-wave anisotropy, ε, using Green River shale as an example. Observe that at high values of ε, the Fresnel-zone diameter at horizontal and near-vertical directions exceeded low ε values by approximately 100%.

This example indicates that if δ^* is negative, the Fresnel-zone diameter at horizontal and near-vertical propagation directions are smaller than those for positive δ^* values, and vice versa. Hence, resolution on horizontal and low-dipping reflectors will be better than that obtained using positive values. The opposite is true for reflectors dipping at intermediate angles.

Effects of variations in γ on Fresnel-zone diameter

Changes in the *SH*-wave anisotropic parameter, γ, also result in significant variations in the curvatures of the shear-wave velocity function, as shown in Figure 8a. Selected values of high and low γ were used in generating the velocity functions and hence the computation of the SH Fresnel-zone diameter. Figure 8b demonstrates the effect of variations in γ on Fresnel-zone sizes. Analysis of this figure indicates that (1) for low values of γ, the changes in Fresnel-zone size with dip will be negligible (hence, lateral resolution will not be expected to change with dip), and (2) if γ is large, the Fresnel-zone varies significantly with dip, and the lateral resolution will change with reflector dip angle due to the velocity function becoming more elliptical.

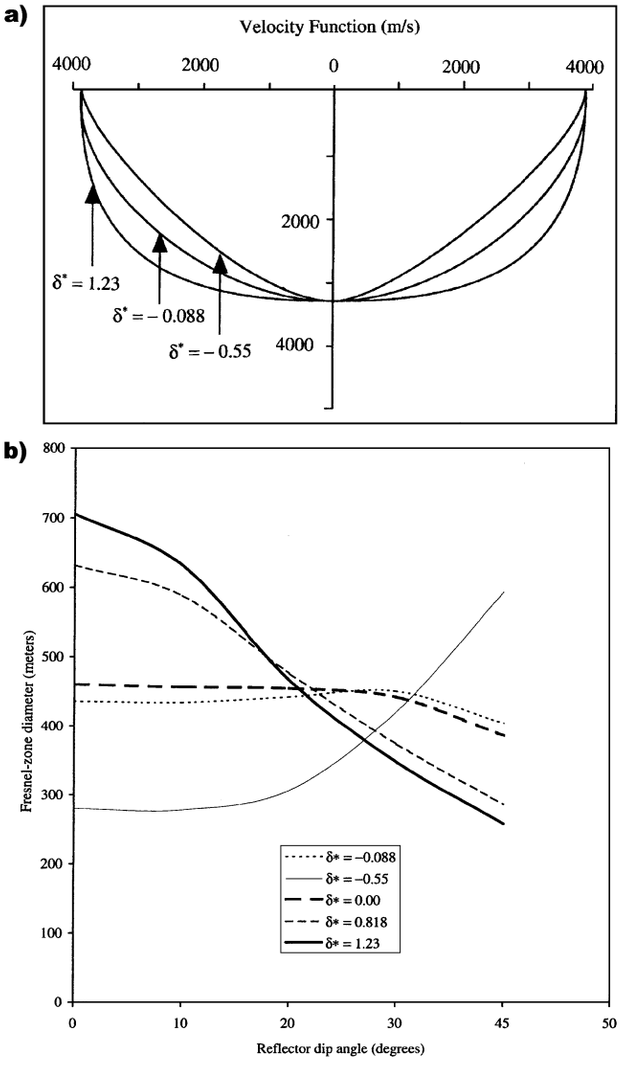

FIG. 7. (a) *P*-ray velocity function shapes in Green River shale for different values of δ^*. This figure indicates changing oblate and narrow width wavefront shapes at horizontal and near-vertical directions for positive and negative δ^* values. (A constant value of $\varepsilon = 0.195$ was used). (b) *P*-wave Fresnel-zone diameter plotted as a function of reflector dip angle for different values of near-vertical *P*-wave anisotropy, δ^*, using Green River shale as an example. When δ^* is negative, the Fresnel-zone diameter at horizontal and near-vertical propagation directions are smaller than those for positive δ^* values. The reverse holds for steeply dipping reflectors.

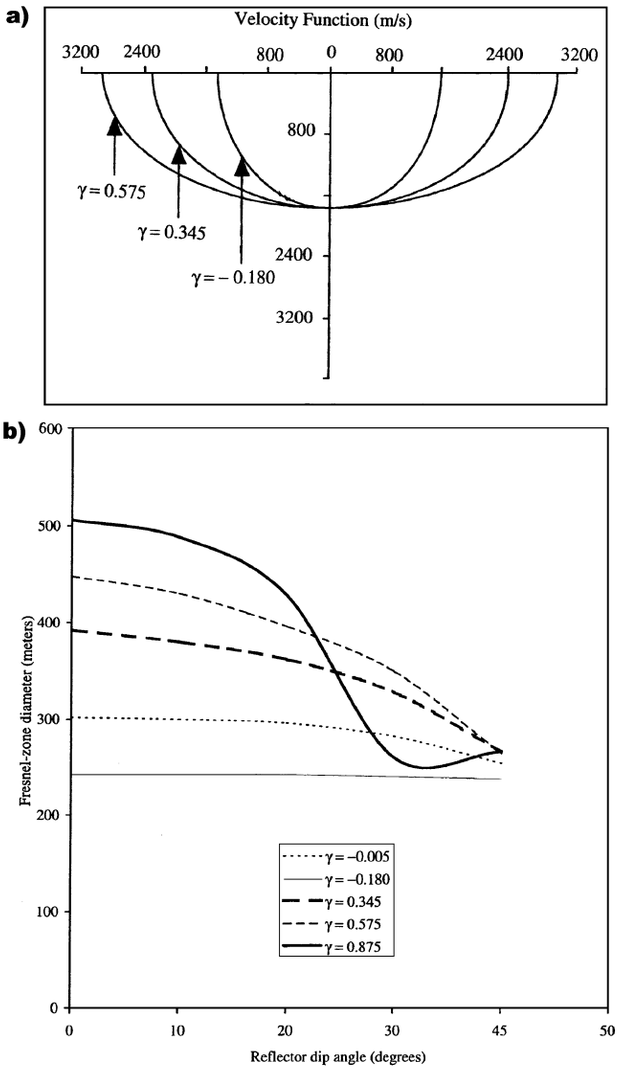

FIG. 8. (a) *SH*-ray velocity function shapes in Green River shale for different values of γ. Variations in γ affect the wavefront shape in all directions. (b) *SH*-wave Fresnel-zone diameter plotted as a function of reflector dip angle for different values of *SH*-wave anisotropic parameter, γ, using Green River shale as an example. If γ is low, the Fresnel-zone diameter exhibits negligible variations with dip. Conversely, if the *SH*-wave anisotropy increases, the Fresnel-zone diameter changes significantly with dip. Note that both positive and negative values of γ are used in this analysis.

Essentially, when the shear wave anisotropy is high, the calculated Fresnel-zone sizes exceeds those of the isotropic case at all reflector dip angles. Hence, the presence of anisotropy is expected to reduce the shear-wave resolving power in all directions.

PHYSICAL MODELING

Physical seismic modeling experiments were also conducted to analyze the effects of anisotropic wavefront curvature and reflector dip angle on spatial resolution. A block of horizontally layered Phenolite laminated plastic, comprising sheets of paper set in phenolic resin, was used to simulate a transversely isotropic medium with a vertical axis of symmetry, similar to the velocity characteristics inherent in shales. This Phenolite material has previously been demonstrated to exhibit transverse-isotrophy symmetry (Okoye and Uren, 1993; Okoye et al., 1996a, b). The model measured 280 mm $\times$ 280 mm $\times$ 780 mm and visually appears to have acceptable degrees of homogeneity. Typical modeling frequencies and velocities generate wavelengths on the order of 3.5 mm. Any inhomogeneities in the modeling materials were far smaller than this.

A dipping layer model (Figure 9) having the same dimensions as the horizontally layered Phenolite block was constructed using the horizontally layered Phenolite material and was used in collecting experimental data for comparison purposes. Since the symmetry axis in this model is tilted with respect to the upper surface of the model, the incident wavefront curvature will be significantly different from those in the horizontally layered model with a vertical axis of symmetry. Cylindrical holes of progressively increasing diameters, each 10 mm deep and flat at the top, were drilled into the bottom of both models. These hole diameters were 25, 35, 40, and 50 mm. These holes served as reflectors, which based on the dominant frequency of the seismic wavelet, represent from 0.20 to 1.43 times the expected Fresnel-zone diameter in Phenolite. A constant offset geometry of 20 mm between the source and receiver, and a station spacing of 2.5 mm was used to collect the reflection data. The acquisition line for all the experiments was centered over the drilled holes. The spatial extents of the reflector boundaries were estimated by marking the half-amplitude points of the horizontal reflector events with respect to the amplitude at the center of the reflectors (Okoye and Uren 1993). The degree of horizontal resolution is determined by comparing the seismically estimated reflector dimension with the true spatial dimension of the reflector. Comparison of the seismically determined reflector sizes from the dipping model with those of the horizontally layered Phenolite model will demonstrate the effects of wavefront curvature and reflector dip angle on resolution.

The scaling factors used in this study were 1:10 000 for both length and time, that is 1 cm and 0.1 μs in the modeling are, respectively, equivalent to 100 m and 1 ms. In order to achieve some random noise reduction in the data, each station was recorded 10 times, permitting a 10-fold vertical stacking when processing the data.

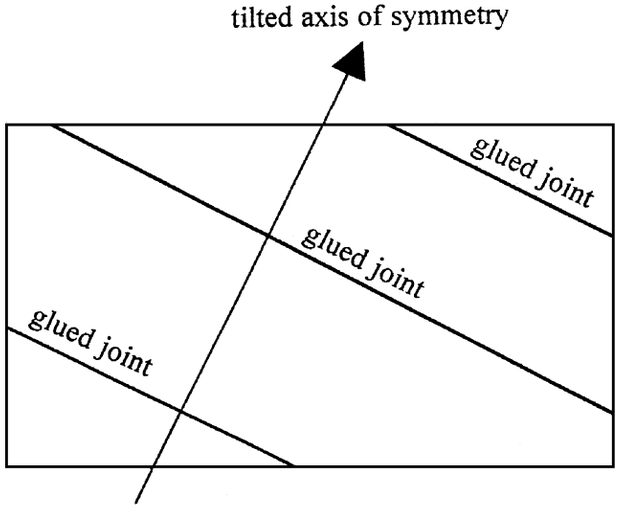

FIG. 9. Phenolite dipping layer model. Paper laminations run parallel to the glued points, thus the axis of symmetry is tilted with respect to the upper surface of the model.

EXPERIMENTAL RESULTS

The effects of inclined anisotropic bedding on the spatial resolution of horizontal events are presented below. This situation may be classified as one of transverse isotropy with the axis of symmetry tilted. To illustrate this effect, seismic section results obtained using the Phenolite dipping layer model are compared with the corresponding results recorded using the horizontally layered model having a vertical axis of symmetry. Both models have the same material composition.

The elastic parameters ε, α_o, and δ^* of the Phenolite material were recovered by an anisotropic inversion technique (Okoye et al., 1996a) and used in calculating the theoretical P-wave velocity function (Figure 10) in the horizontally layered Phenolite model. This Phenolite material has been determined experimentally to be transversely isotropic since the velocities measured at azimuths perpendicular to the symmetry axis are almost equal. Because of the tilt of the symmetry axis, the curvature of the wavefront in the dipping layer model impinging on the reflectors is broadened as compared to that in horizontally layered medium.

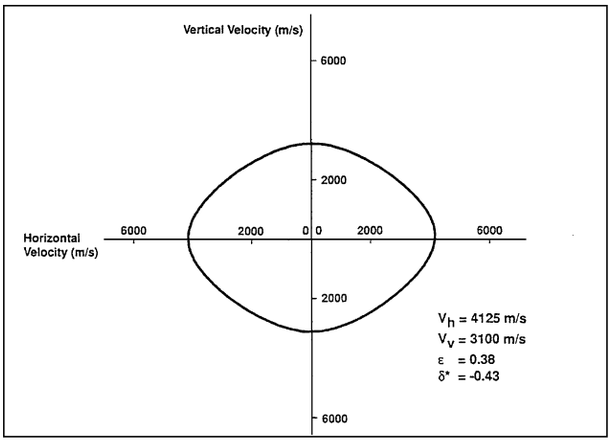

FIG. 10. Calculated theoretical P-ray velocity function in the horizontally layered Phenolite model. Due to the negative value of δ^*, the wavefront curvature at horizontal and near-vertical directions is concave.

Figure 11 shows *P*-wave data recorded in dipping layered and horizontally layered Phenolite models for reflector diameters of 25 mm (250 m) and 35 mm (350 m). While the true lateral extent of the reflectors in the dipping layered model is overestimated by approximately 51%, it is misrepresented by about only 20% in the horizontally layered model. The varying degrees of resolution observed in this example are due to the different wavefront curvatures incident on the reflectors in the two media.

Similarly, for reflector diameters of 40 mm (400 m) and 50 mm (500 m) in both models, spatial imaging of the reflector dimensions are better achieved in the horizontally layered model (Figure 12a) compared to the dipping layer model (Figure 12b). While the true reflector dimensions are overestimated by about 22% in the medium with a vertical axis of symmetry, they are misrepresented by approximately 45% in the medium with a tilted axis of symmetry because of the resultant variations in wavefront curvatures.

Shear-wave seismic data recorded for reflector diameters of 25 mm and 35 mm in the dipping layer model and diameters of 25 mm, 35 mm, and 45 mm in the horizontally layered model are shown in Figure 13. Despite the small variations in curvatures of the *SH*-wavefront incident on the reflectors in these two media, the differences in the lateral resolution of the reflector events are fairly significant as indicated in the section results. Again the lateral resolving power of the shear wave is seen to be better in the horizontally layered medium with a slightly more concave wavefront shape compared to that of the dipping layer model having a less concave wavefront curvature. While the true spatial extent of the reflectors in the horizontally layered model is overestimated by about 27%, it are misrepresented by approximately 50% in the dipping layer model.

Figure 14a and 14b show *SH* data recorded for reflector diameters of 40 mm and 50 mm in both models, respectively. Similarly the seismic reconstruction of the spatial extent of the reflectors is better achieved in the horizontally layered Phenolite model compared to the dipping layer model. Apparent overestimation of the true reflector diameters occured by approximately 29% in the horizontally layered model and by about 57% in the dipping layer model.

The above examples indicate that when a medium is anisotropic and the axes of velocity symmetry are tilted with respect to the horizontal, the spatial imaging of horizontal reflection events is significantly affected by the dip angle of the bedding and hence the resultant wavefront shape incident on the reflector.

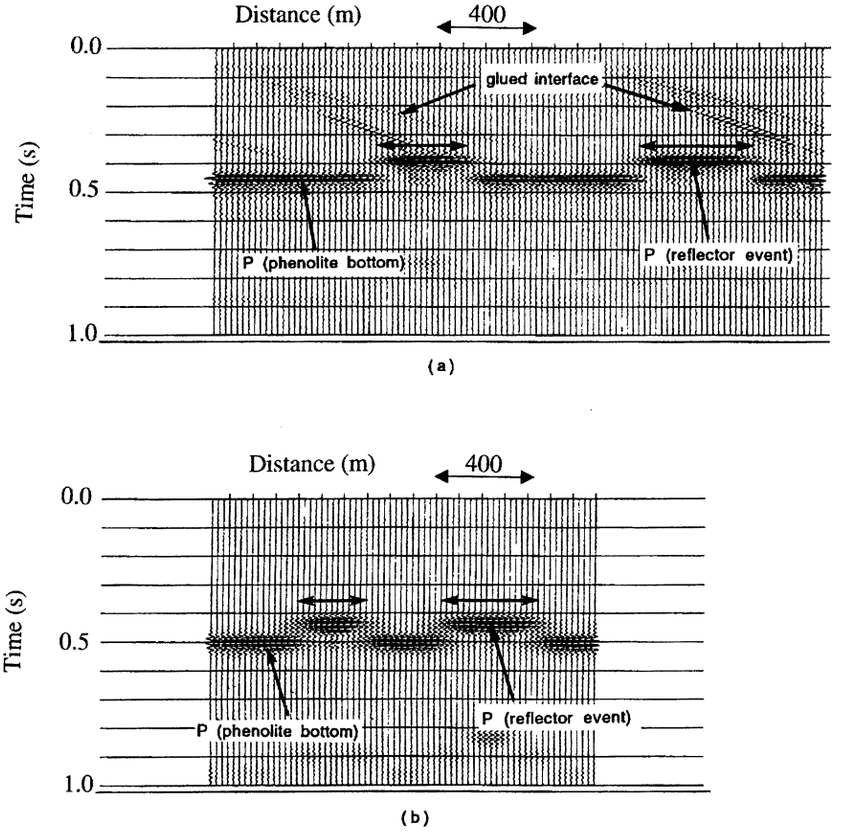

FIG. 11. *P*-wave data recorded for reflector diameters of 25 mm (250 m actual size) and 35 mm (350 m actual size) in Phenolite: (a) dipping layered and (b) horizontally layered. Due to the different wavefront curvatures incident on the reflectors in these two media, the resolution of the horizontal extent of the reflectors in each medium is significantly different. Resolution of the reflector extents is worse by about 51% in the dipping layered model and by about 20% in the horizontally layered model.

CONCLUSIONS AND DISCUSSION

This study shows the effects of velocity anisotropy on Fresnel-zone diameter and hence spatial resolution, a phenomenom of vital importance in interpreting seismic reflection data.

Considerable differences exist between the Fresnel-zone diameter for anisotropic and isotropic velocity functions depending on reflector dip. The spatial resolution obtained for an anisotropic medium is therefore significantly different from that determined for the same medium if it is (as in most surface seismic field studies) assumed to be isotropic.

The anisotropic reflection isochrons have complex shapes which vary with dip and are nonsymmetric in nature. The asymmetric nature of the reflection patterns suggest that, in the presence of anisotropy, the shape of the Fresnel zone and hence spatial resolution will vary with reflector dip angle. In addition, the contribution to the total reflected energy arising from the reflecting zone may be unequally distributed with respect to the geometrical reflection point.

Numerical studies strongly indicate that Fresnel-zone diameter and hence spatial resolution in anisotropic media are affected by the elastic parameters ε, δ^*, and γ, which characterize the nature of the anisotropic wavefront for *P*- and *SH*-waves. *P*-wave resolution on a horizontal reflector may be increased or reduced depending predominantly on the value and sign of the elastic parameter δ^*. In every case, shear-wave spatial resolving power is reduced by anisotropy caused by sedimentary layering compared to that in isotropic media.

Physical modeling studies have demonstrated that anisotropy can significantly affect the spatial resolving power of seismic waves. The magnitude of these effects depends on the curvature of the wavefront, which changes with dip and orientation of the symmetry axis.

The findings of this study on spatial resolution are only applicable to unmigrated seismic data. The implementation of a properly formulated 3-D anisotropic migration scheme will improve spatial resolution. The improvement factor in spatial resolution afforded by optimum migration is the ratio of the premigration Fresnel diameter to the postmigration diameter. However, if a 2-D migration process is used, which is often the case, the improvement in resolution will be effective only in the direction of profile, and the Fresnel diameter is only reduced in this direction (Lindsey, 1989). Hence, the postmigrated Fresnel-zone shape will be elliptical, with the major axis perpendicular to the seismic profile and equal to the premigration Fresnel diameter, while the minor axis in the profile direction equals the postmigrated and reduced Fresnel diameter.

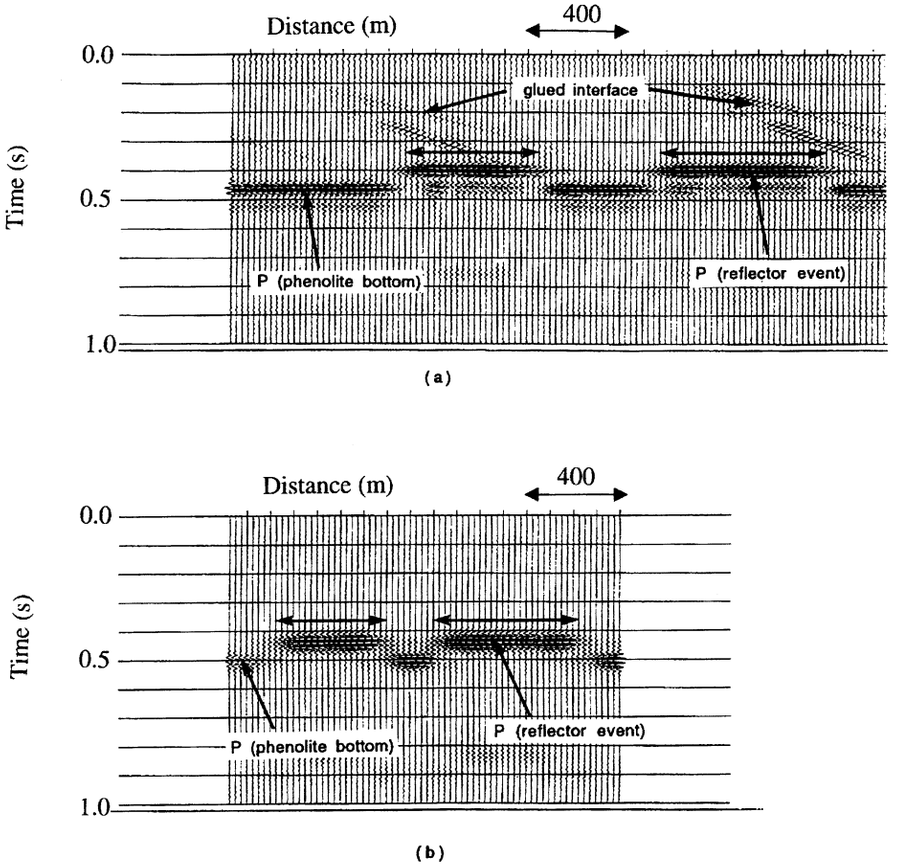

FIG. 12. *P*-wave data recorded for reflector diameters of 40 mm (400 m actual size) and 50 mm (500 m actual size) in Phenolite: (a) dipping layered and (b) horizontally layered. Again, the spatial dimension of the reflectors are poorly resolved in (a) than in (b). Overestimation of the reflector dimensions occurred by about 45% in the dipping layered model and by about 22% in the horizontally layered model.

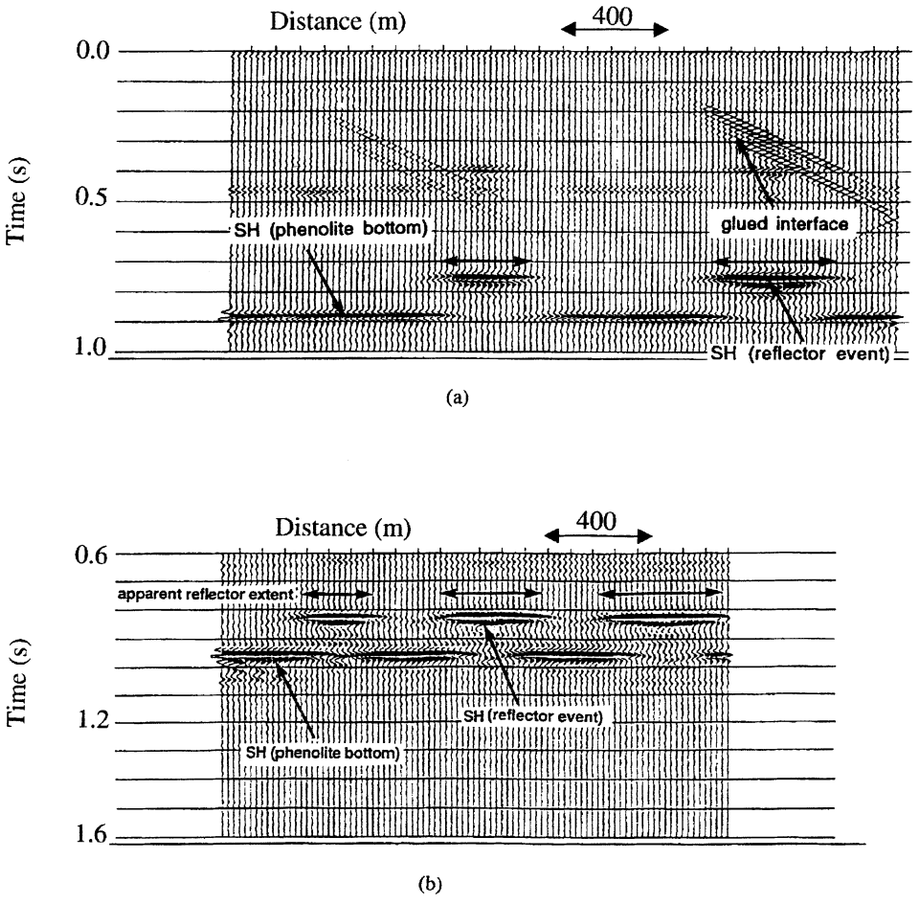

FIG. 13. *SH*-wave data recorded in (a) dipping layered Phenolite for reflector diameters of 25 mm (250 m actual size) and 35 mm (350 m actual size), and (b) horizontally layered Phenolite for reflector diameters of 25 mm (250 m actual size), 35 mm (350 m actual size), and 45 mm (450 m actual size). Observe again the poor spatial reconstruction of the reflector extent by shear waves in the dipping layered medium compared to that in the horizontally layered medium. While the true spatial dimension of the reflectors is overestimated by about 50% in (a), it is misrepresented by approximately 27% in (b).

ACKNOWLEDGMENTS

This is a project in the Geophysics program of the Australian Petroleum Cooperative Research Center (APCRC). The authors thank Dr. Bruce Hartley for a critical review of this manuscript during its preparation. We also acknowledge the contributions of Prof. Shuquan Guo in software development. Fruitful discussions with Mohamad Nasser Ismail are also appreciated.

REFERENCES

Asatryan, A. A., and Kravtsov, Y. A., 1988, Fresnel zones of hyperbolic type from the physical point of view: Wave Motion, **10**, 45–57.
Dellinger, J., and Muir, F., 1988, Imaging reflections in elliptically anisotropic media: Geophysics, **53**, 1616–1618.
Eaton, D. W. S., Stewart, R. R., and Harrison, M. P., 1991, The Fresnel zone for *P-SV* waves: Geophysics, **56**, 360–364.
Lindsey, J. P., 1989, The Fresnel zone and its interpretive significance: The Leading Edge, **8**, No. 10, 33–39.
Okoye, P. N., 1995, Seismic reflection process in anisotropic media: PhD thesis, Curtin Univ. of Technology.
Okoye, P. N., and Uren, N. F., 1993, Spatial resolution and amplitude studies in anisotropic seismic reflection: A physical modelling study: Expl. Geophys., **24**, 751–760.
Okoye, P. N., Uren, N. F., McDonald, J. A., and Ebrom, D. A., 1996b, Variation of spatial resolution with orientation of symmetry axis in anisotropic media, *in* Erling, F., Rune, M. H., and Jaswant, S. R., Eds., Seismic anisotropy: Soc. Expl. Geophys.
Okoye, P. N., Zhao, P., and Uren, N. F., 1996a, Inversion technique for recovering the elastic constants of transversely isotropic materials: Geophysics, **61**, 1247–1257.
Sheriff, R. E., 1980, Nomogram for Fresnel zone calculation: Geophysics, **45**, 968–972.
Thomsen, L., 1986, Weak elastic anisotropy: Geophysics, **51**, 1954–1966.

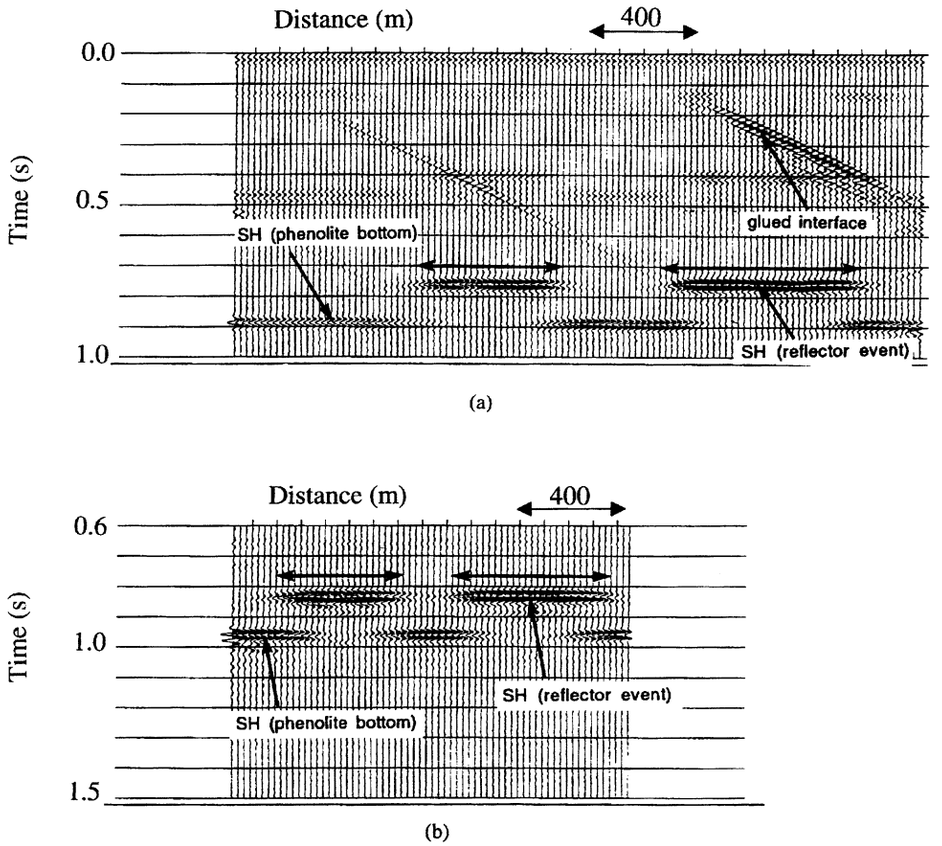

FIG. 14. *SH*-wave data recorded for reflector diameters of 40 mm (400 m actual size) and 50 mm (500 m actual size) in Phenolite: (a) dipping layered and (b) horizontally layered. Similarly, the spatial dimension of the reflectors are more poorly resolved in (a) than in (b). Overestimation of the reflector dimensions occurred by about 57% in the dipping layered model and by about 29% in the horizontally layered model.